Int. J. Electrochem. Sci., 7 **(2012)** 3773 - 3786

International Journal of
ELECTROCHEMICAL
SCIENCE
www.electrochemsci.org

Effect of NaCl on the Corrosion of Cold Rolled Steel in Peracetic Acid Solution

Lei Li[1], *Qing Qu*[2,*], *Wei Bai*[3], *Yajun Chen*[2], *Shiwen Zhang*[2], *Gengrui Gao*[2], *Zhongtao Ding*[2]

[1] Laboratory for Conservation and Utilization of Bio-Resources, Yunnan University, Kunming 650091, China
[2] School of Chemical Science and Technology, Yunnan University, Kunming 650091, China
[3] Department of Chemistry, Yunnan Nationalities University, Kunming 650092, China
[*]E-mail: quqing58@yahoo.com.cn

Received: 6 January 2012 / *Accepted:* 16 February 2012 / *Published:* 1 April 2012

Effect of sodium chloride (NaCl) on the corrosion of cold rolled steel (CRS) in peracetic acid solution (PAA) was investigated by potentiodynamic polarization curves, cyclic polarization curves and electrochemical impedance spectroscopy (EIS) at 0 °C, 10 °C, 20 °C, 30 °C and 40 °C, respectively. The results show that concentrations of NaCl and test temperatures can affect the corrosion rate clearly. At each same temperature, the corrosion rate firstly increases with increasing NaCl concentration up to 0.005 M, and then slightly decreases in solution with NaCl level higher than the threshold value. The corrosion increases with increasing the temperature at each same concentration of NaCl. Potentiodynamic polarization and cyclic polarization curves indicate that no obvious pitting occurs in the process.

Keywords: corrosion; peracetic acid; NaCl; cold rolled steel

1. INTRODUCTION

As a strongly oxidizing acid, peracetic acid (PAA) has a long history of usage as disinfectants and sterilizers due to its microbicidal activities [1–2]. PAA is also one of the few treatment products approved for sanitizing foods carrying the organic label [3]. Interest is growing for its use as a green alternative to chlorination for water treatment [4,5]. However, major disadvantages associated with PAA disinfection are the serious economic loss due to its highly corrosive capability to any metals that are used in some appliances. Thus, corrosion problem to metal materials caused by PAA has been attracted more attentions [6–9]. Pehkonen et al. [6] have investigated corrosion of stainless steels in ozone and peracetic acid, their results showed that the corrosion rates in PAA solutions were lower than in ozone solutions, they deemed the corrosion behavior of stainless steel in PAA was unknown.

Qu et al. [7] studied the corrosion behavior of cold rolled steel (CRS) in PAA solutions by polarization curve method; they suggested the adsorption of PAA on the surface of CRS was an important factor on the corrosion. Furthermore, Qu et al. [8, 9] also studied the corrosion of CRS in PAA containing molybdate and tungstate, their results indicate that addition of molybdate and tungstate in PAA can retard the corrosion of CRS clearly. Other studies about the corrosion behavior of carbon steel in PAA solutions are very scant.

Generally speaking, only extremely low concentrations of PAA (0.1 - 0.5 % by weight) can be used for disinfection, so dilution of PAA by a lot of water before use is necessary. However, chloride ions are inevitable not only in natural water such as river water, sea water, underground water but in much domestic water. That is, PAA disinfectant may possess chloride ions. It is well known that chloride ions have an important role in the corrosion of metals in different media. And a number of investigations have been devoted to the effects of chloride ions on the corrosion of metals [10-18]. Many investigations reveal that chloride ions can accelerate the corrosion of steel, especially cause the localized corrosion [10-15]. On the other hand, some researches also indicate that chloride ions also can weaken the corrosion of steel in some special environments [16-18]. The results of Hackerman et al. [16] and Li et al.[17] show that single chloride ions can inhibit steel corrosion somewhat in acid solutions attributed to the strong adsorption of chloride ions on iron surface. Lee et al. [18] studied the influence of groundwater anions on the impedance behaviour of carbon steel corroding under anoxic conditions, their results indicate that in Cl^--dominated solutions when other anions, especially CO_3^{2-}/HCO_3^-, are absent, corrosion is extremely slow and the steel appears passive. However, literature available to date on the corrosion mechanism of metals in PAA containing chloride is very scant; the role of chloride ions on the corrosion of steel in PAA is unknown.

The objective of this investigation is to determine the effect of chloride ions on the corrosion of cold rolled steel (CRS) in 0.5 % PAA by weight solution. A probable inhibitive mechanism is presented to explain the experimental observations.

2. EXPERIMENTAL METHOD

2.1. Materials

The working electrodes were made of a sheet of cold rolled steel (CRS), which was of commercial specification with composition (wt%): C ≤ 0.05, Si ≤ 0.02, Mn ≤ 0.28, S ≤ 0.023, P ≤ 0.019, Fe remainder.

2.2. Solutions

The aggressive solution, 0.5% PAA by weight, was prepared by dilution of 18.4% PAA by weight. Sodium chloride (NaCl) used were of analytical grade. All solutions were prepared from distilled water.

2.3. Electrochemical measurements

A three-electrode system including a working electrode, an auxiliary electrode and a reference electrode was used for the electrochemical measurements in 250 mL solution. The working electrodes were made of CRS which were embedded in PVC holder using epoxy resin with a square surface of 1.0 cm^2. The auxiliary electrode was a platinum foil. The reference electrode was a saturated calomel electrode (SCE) with a fine Luggin capillary positioned close to the working electrode surface in order to minimize ohmic potential drop. Each specimen was successively abraded by using SiC emery papers from 100 to 1000 grades on the test face. Before use, the abraded surface was thoroughly washed with distilled water and degreased in acetone then dried with a warm air stream. The working electrode was immersed in the test solution at open circuit potential for 2 h before measurement until a steady state appeared. The potentiodynamic polarization curves were carried out by polarizing in the range between -250 and 1600 mV with respect to Ec vs. SCE at a scan rate of 1 mV s^{-1}. And the cyclic polarization curves were performed by polarizing to ± 250 mV with respect to the free corrosion potential (Ec vs. SCE) at a scan rate of 0.5 mV s^{-1}. A 10 mV peak to-peak sine wave over an ac frequency range extending from 0.1 Hz to 100 kHz was used for the impedance measurements. All electrochemical measurements were carried out at the open circuit potential using PARSTAT 2263 Potentiostat/Galvanostat (Princeton Applied Research). Each experiment was repeated at least three times to check the reproducibility. All tests have been performed in non-deaerated solutions under unstirred conditions at 0 - 40 ˚C.

3. RESULTS AND DISCUSSION

3.1 Potentiodynamic polarization curves

The potentiodynamic polarization curves for CRS in PAA solutions without and with NaCl after 2 h immersion at 20 ˚C were shown in Fig.1. The polarization curves at other temperatures are the same as those at 20 ˚C and not presented here. As can be seen from Fig.1, comparing with that in PAA without NaCl, the corrosion potentials in the presence of NaCl are shifted to more negative direction, the cathodic branches are shifted to positive potential direction and the anodic branches are shifted to negative potential direction, accordingly, the cathodic and anodic current densities also increase, suggesting that chloride ions accelerate both the anodic and cathodic reactions. Furthermore, it is easy to see from Fig.1 that, with increasing concentration of NaCl in the range 0 to 0.005 M, the anodic current densities increase noticeably, but when the concentration is higher than 0.005 M, the anodic current densities is lower than that of 0.005 M, which indicates that the maximum acceleration of the anodic reaction occurs in PAA containing 0.005 M NaCl.

To investigate the effect of temperature on the corrosion, the potentiodynamic polarization curves for CRS in PAA containing 0.005 M Cl^- were carried out and recorded in Fig.2. From Fig.2 it is easy to see that, with increase of the temperature, the anodic branches are shifted to negative potential direction obviously, suggesting that the anodic dissolution of CRS increases with increase the temperature. On the contrary, the cathodic branches shift to positive direction unclearly; this indicates that increase of the corrosion rate with increase of the temperature is mainly due to acceleration of anodic dissolution.

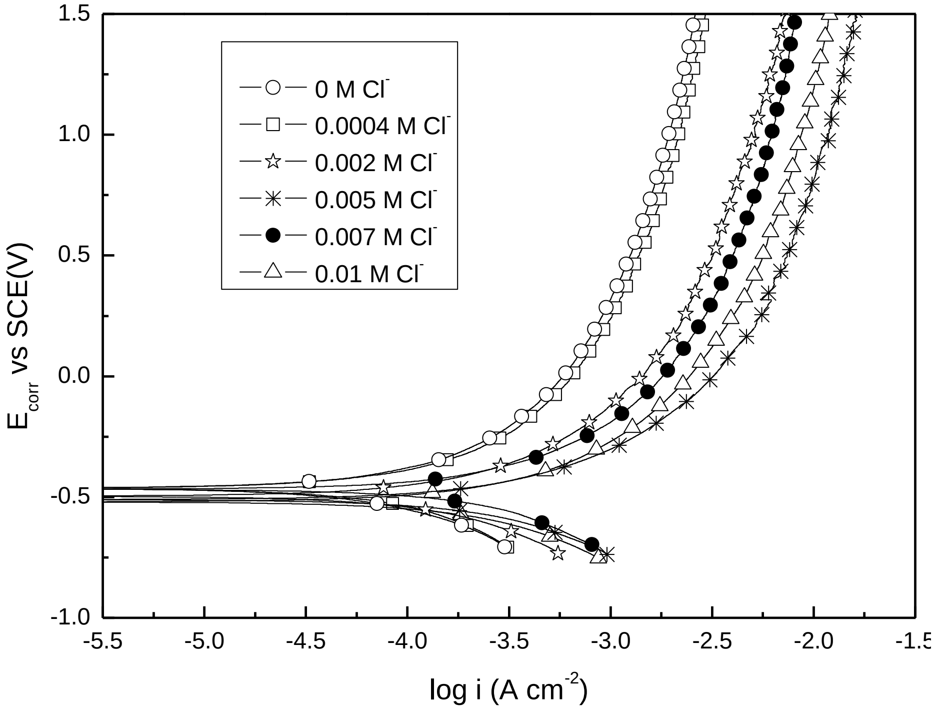

Figure 1. Potentiodynamic polarization curves for CRS in PAA solution with and without NaCl at 20 ˚C.

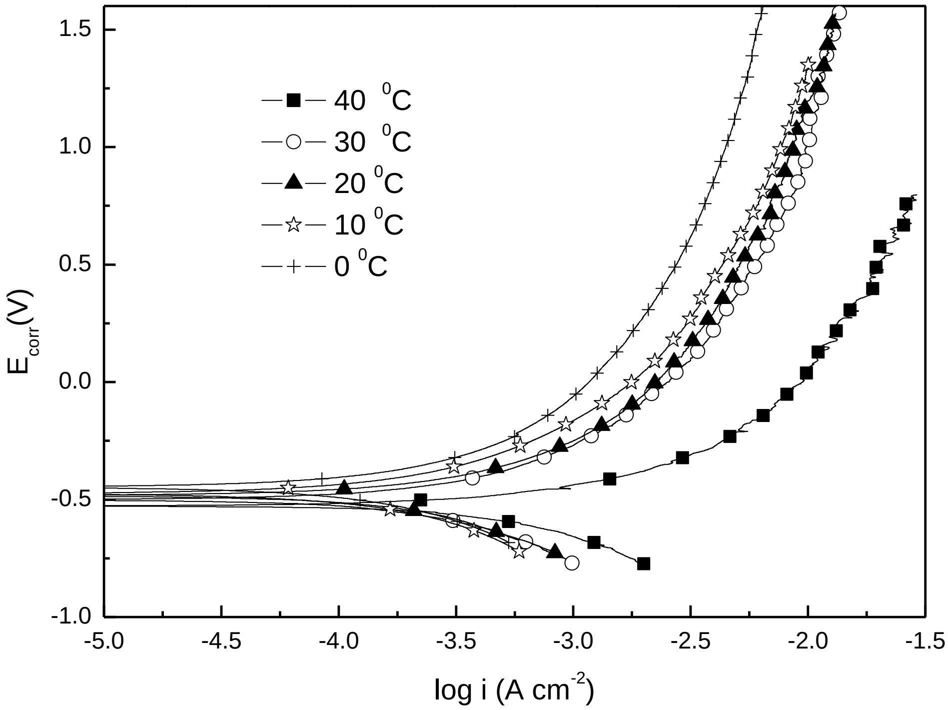

Figure 2. Potentiodynamic polarization curves of CRS in PAA containing 0.005 M NaCl at different temperatures.

It also can be seen from Fig.1 and 2 that polarization curves do not show sufficient linear Tafel regions. The distortion of the polarization curves is mainly caused by the solution resistance (solution ohmic drop) [19-21]. In order to obtain meaningful data, it is necessary to perform an appropriate correction of polarization curves before the Tafel plot analysis. The correction of polarization curves for ohmic drop was well performed according to the method described in literatures [9, 19-21] assuming that the experimentally applied overpotential at any current is given by the following equation:

$$E = \beta_a + \beta_c \ln i + iR_s \qquad (1)$$

where E is the applied overpotential vs. SCE, i the current density, R_s the solution resistance and β_a and β_c are respectively anodic and cathodic Tafel slopes.

Using the relationship (1), the following equation for correction of the polarization curves for ohmic drop can be obtained [22]:

$$i = i_{corr}\left[\exp\left(\frac{E - E_{corr} - iR_s}{\beta_a}\right) - \left(-\frac{E - E_{corr} - iR_s}{\beta_c}\right)\right] \qquad (2)$$

where i_{corr} is the corrosion current density, E_{corr} the corrosion potential vs. SCE and S is the area of the exposed surface of the working electrode in cm^2. And the solution resistance (R_s) used in this paper is derived from EIS method which provides a variety of information on the parameters of the electrochemical cell and can be profitably used to determine the solution resistance [23]. According to Eq.(2), more powerful non-linear least squares algorithm based on the Levenberg-Marqurdt Method (LEV) was used to fit the experimental data to obtain the corrosion current density (Icorr), Tafel slopes β_a and β_c.

To enhance the quality of fit, the data rage is set within E_{corr} vs. SCE ± 150 mV, the initial values of E_{corr}, I_{corr}, β_a and β_c are set to 0 V, 10^{-5} A cm^{-2} and 120 mV $decade^{-1}$, respectively. Rather than giving equal importance to each data point, data points below the current accuracy which is chosen as 1×10^{-5} A m^{-2} in this paper have reduced importance in the overall goodness of fit. This causes the fit to place a higher importance on the data points with larger currents. In all cases, the above method fits the experimental curves well after correction for ohmic drop in the selected range, with a regression coefficient (R^2) > 0.90.

The potentiodynamic polarization parameters after correction for ohmic drop including E_{corr}, I_{corr}, β_a and β_c were listed in table 1.

From table 1 it can be seen that, the corrosion current densities obviously increase with increasing the concentration of NaCl from 0 to 0.0005 M, and then they will decrease from 0.005 to 0.01 M. That is, the maximum corrosion occurs at 0.005 M at each same temperature. At the same concentration the current densities also increase with increase of the temperature.

Table 1. Electrochemical corrosion parameters obtained from potentiodynamic polarization curves for CRS in PAA solution with and without NaCl

T (℃)	C(mol/L) Cl^-	β_{ca} (mV/deg)	β_{an} (mV/deg)	E_{corr} (V)	I_{corr} (μA /cm^2)
0	0	687.9	516.3	-403.5	282.7
0	0.0004	965.5	863.7	-432.7	336.5
0	0.002	937.4	690.4	-447.7	396.7
0	0.005	857.8	480.6	-472.3	455.6
0	0.007	833.3	483.5	-432.7	448.8
0	0.01	640.0	317.4	-464.6	432.6
10	0	491.8	915.3	-446.4	307.5
10	0.0004	1050	813.0	-477.2	349.6
10	0.002	1065	726.8	-474.7	454.6
10	0.005	673.9	470.9	-508.2	495.1
10	0.007	784.2	647.9	-506.8	473.8
10	0.01	479.0	320.9	-515.8	473.1
20	0	1529	1189	-462.5	379.0
20	0.0004	1055	996.9	-510.4	472.5
20	0.002	896.4	574.3	-510.4	522.6
20	0.005	887.9	463.9	-510.7	597.1
20	0.007	554.0	331.5	-529.7	550.6
20	0.01	568.8	498.2	-520.4	556.6
30	0	1293	1182	-428.4	487.6
30	0.0004	1019	983	-527.9	496.0
30	0.002	901.1	713.5	-504.9	632.5
30	0.005	1106	615.0	-480.8	757.2
30	0.007	903.1	497.7	-461.7	749.9
30	0.01	785.4	347.1	-472.2	742.6
40	0	948.4	829.5	-424.3	578.3
40	0.0004	878.0	640.5	-545.3	615.0
40	0.002	762.5	399.7	-575.4	704.4
40	0.005	614.5	338.6	-530.6	854.7
40	0.007	756.1	468.4	-543.9	853.7
40	0.01	450.9	181.6	-549.1	847.2

3.2 Cyclic polarization curves

Fig.1 also indicates that addition of NaCl to PAA solution does not affect the shape of the anodic polarization curve, the anodic current density increases with the applied potential regularly both in PAA with and without NaCl, suggesting that no obvious pitting occurs in the dissolution of CRS.

In order to further confirm this result, the cyclic polarization technique, which is normally used to qualitatively evaluate a metal’s tendency to pit in a corrosive environmental, was used to determine the susceptibility to pitting in PAA containing NaCl. Fig.3 gives the cyclic polarization curves in PAA without and with 0.005 M NaCl at 20 °C, the curves elucidate that reverse sweeps overlap with the forward ones in principle, that is, no significant positive or negative hysteresis are observed in these curves, suggesting only active corrosion takes place in the dissolution of CRS in PAA without and with NaCl, namely, chloride ions do not provoke the pitting corrosion of CRS in PAA solution.

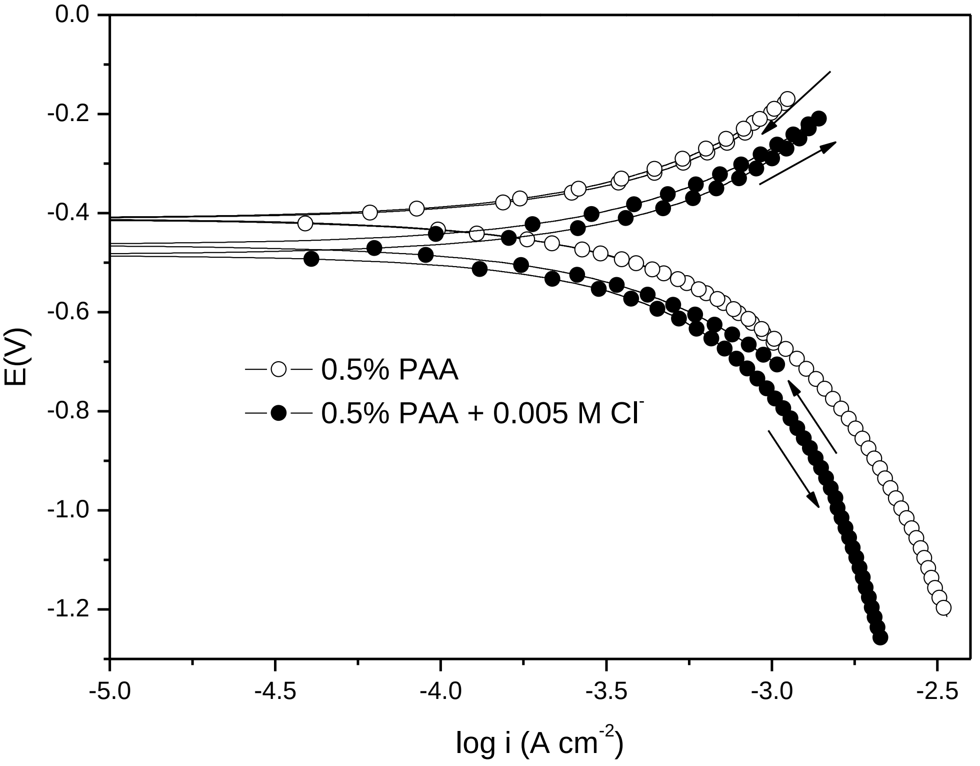

Figure 3. Cyclic polarization curves in PAA without and with 0.005 M NaCl at 20 °C.

3.3 EIS results

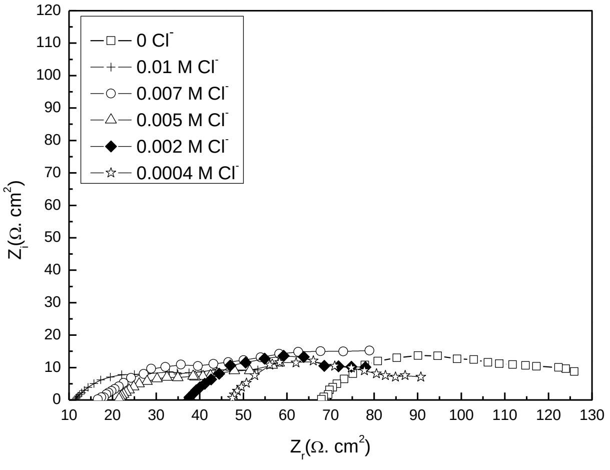

Figure 4. EIS of CRS in PAA with and without NaCl at 20 °C.

A better understanding of the mechanism operating at the electrode surface was attained through EIS measurements at the corresponding corrosion potential. All the impedance measurements were performed and recorded in Nyquist plots in this study. Nyquist plots of CRS in PAA with and without NaCl at 20 °C after 2 h immersion were given in Fig. 4. The Nyquist plots at other temperatures are the same as those at 20 ˚C and not presented here. All impedance spectra exhibit part of a single depressed semicircle. These depressed incomplete semicircles can be attributed to the charge transfer that takes place at electrode/solution interface, and the transfer process controls the corrosion reaction of CRS [24]. Fig.4 also shows that the presence of NaCl can not affect the appearance of the Nyquist plots of CRS in PAA solution, suggesting that the presence of NaCl does not change the mechanism of dissolution [24, 25]. Comparing the depressed semicircles in the presence of NaCl with that in the absence of NaCl, it is easy to see that the capacitance loops in the presence of NaCl are bigger than that in the absence of NaCl, which suggests that NaCl can promote the corrosion performance of PAA.

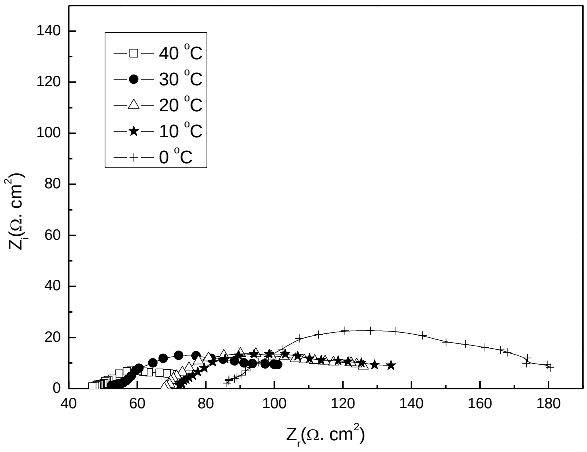

Figure 5. EIS of CRS in PAA solution containing 0.005 M NaCl at different temperatures.

Fig.5 gives the Nyquist plots of CRS in PAA containing 0.005 M NaCl at different temperatures. It is clear that the temperature does not affect the appearance of the impedance in PAA with NaCl, and the size of the capacitance loops decreases with increasing the temperature. That is, the corrosion increases with increasing the temperature, and variation in temperature does not change the mechanism of dissolution of CRS too.

From the Nyquist plots it also can be seen that the high frequency limit of the impedance, which can be attributed to the solution resistance, increases with decrease of the NaCl concentration and the temperature, since it is shifted to higher values on the Zreal axis. Namely, the conductivity of the solution which is reverse to the solution resistance increases with increase in concentration and temperature.

The EIS results were simulated using the equivalent circuit shown in Fig.6 to pure electronic models that could verify or role out mechanistic models and enable the calculation of numerical values corresponding to the physical and/or chemical properties of the electrochemical system under investigation [26].

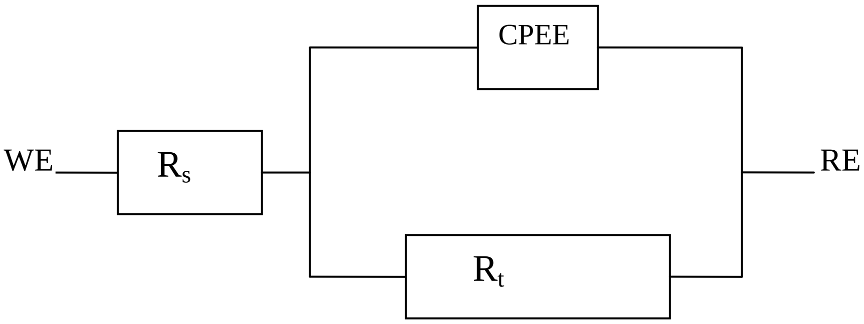

Figure 6. Equivalent electrical circuit of EIS.

Table 2. Electrochemical parameters from EIS for CRS in PAA solution with and without NaCl.

T (℃)	Cl^- (mol/L)	R_s (Ω cm^2)	R_t (Ω cm^2)	C_{dl} (μF·cm^2)	α
0	0	86.7	117.7	913	0.652
0	0.0004	64.6	108.0	1011	0.641
0	0.002	43.8	99.69	1078	0.638
0	0.005	28.6	77.33	1390	0.629
0	0.007	21.9	80.56	1334	0.617
0	0.01	16.8	80.55	1231	0.615
10	0	72.3	113.1	1069	0.688
10	0.0004	51.7	101.2	1195	0.679
10	0.002	43.4	72.82	1661	0.653
10	0.005	24.7	61.93	1953	0.648
10	0.007	20.4	74.33	1627	0.635
10	0.01	14. 8	71.72	1686	0.641
20	0	67.9	90.47	1844	0.679
20	0.0004	47.5	88.34	2043	0.681
20	0.002	37.6	65.06	2890	0.657
20	0.005	21.5	45.62	2772	0.652
20	0.007	16.6	53.63	2380	0.633
20	0.01	11.5	52.52	2430	0.651
30	0	52.5	65.52	2819	0.711
30	0.0004	39.3	57.41	2941	0.685
30	0.002	24.7	55.43	3262	0.662
30	0.005	17. 1	43.44	4162	0.656
30	0.007	10.7	49.97	3618	0.649
30	0.01	8.7	49.17	3677	0.591
40	0	46.8	56.17	2907	0.735
40	0.0004	27.2	48.47	3369	0.714
40	0.002	19.4	44.17	3697	0.688
40	0.005	12.4	40.26	4056	0.674
40	0.007	8.3	46.46	3505	0.659
40	0.01	6.6	45.85	3561	0.650

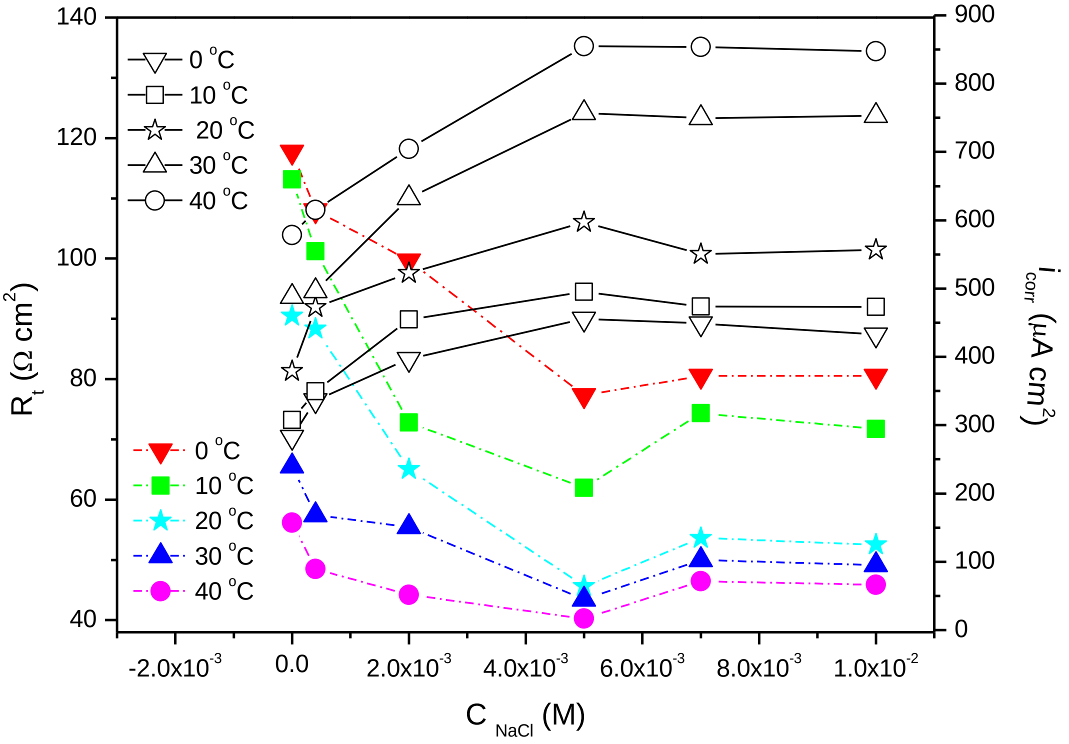

Figure 7. Relationship between charge transfer resistance (R_t) and corrosion current density (i_{corr}) as a function of concentrations of NaCl (C_{NaCl}). (solid symbols: R_t , open symbols: i_{corr}).

The circuit employed allows the identification of both solution resistance (R_s) and charge transfer resistance (R_t). It is worth mentioning that the double layer capacitance (C_{dl}) value is affected by imperfections of the surface, and that this effect is simulated via a constant phase element (CPE) [27,28].

A constant phase element composed of a component Q_{dl} and a coefficient α is required, and α quantifies different physical phenomena like surface inhomogeneousness resulting from surface roughness, inhibitor adsorption, porous layer formation, etc. So the capacitance is deduced from the following relation [28]:

$$C_{dl} = Q_{dl} \times (2\pi f_{\max})^{\alpha-1} \qquad (3)$$

where $f_{\max}$ represents the frequency at which imaginary value reaches a maximum on the Nyquist plot. If the electrode surface is homogeneous and plane, α is equal to 1 and the electrode surface can be treated as an ideal capacitance.

Parametrical adjustment of this circuit with experimental impedance spectra gives access to the double layer capacitance and charge transfer resistance. R_s, R_t, C_{dl} and α fitted from EIS in different concentrations of PAA at test temperatures were listed in Table 2. As can be seen from Table 2, R_t decrease while C_{dl} increases with increase of temperatures of PAA at each NaCl concentration, but R_t and C_{dl} do not always decrease or increase with increase of concentrations of NaCl at the same temperature, the turning points appear in the presence of 0.005 M NaCl. This further reveals that the maximum corrosion of CRS occurs in the presence of 0.005 M NaCl. The change in C_{dl}, which can result from a change in local dielectric constant and/or an increase in the thickness of the electrical double layer, suggests that PAA functions by adsorption at the metal solution/interface [29]. From table 2, it is also to see that the C_{dl} values of CRS in the presence of NaCl are bigger than that in the absence of NaCl at each same temperature, indicating that NaCl can hinder the adsorption of PAA on CRS due to the competitive adsorption between Cl^- and $CH3COOO^-$.

Fig.7 compares i_{corr} with R_t as a function of concentration of NaCl. As it can be seen from this figure that, at each temperature, i_{corr} increases while R_t decreases with increases of concentration of NaCl from 0 to 0.005 M, then, i_{corr} decreases while R_t increases somewhat with increase of the concentration of NaCl from 0.005 to 0.01, that is, the corrosion rate firstly increases with increasing chloride content up to a certain critical concentration (0.005 M), and then decreases in solution with chloride level higher than the threshold value. At each same concentration of NaCl, i_{corr} increases while R_t decreases with increases of temperature from 0 to 40 ˚C. Namely, the results obtained from EIS are in good agreement with the polarization studies, all the result elucidate that temperatures and concentrations of NaCl fundamentally affect the corrosion of cold rolled steel in PAA solution.

4. DISCUSSION

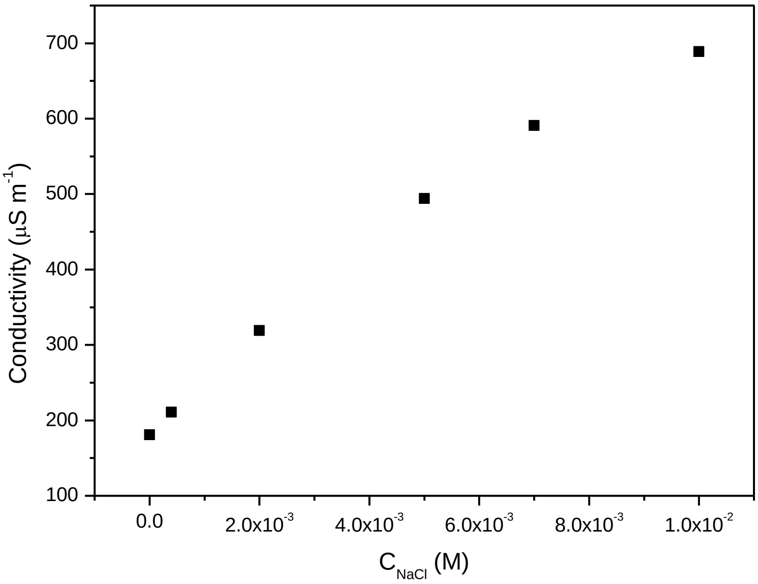

Figure 8. Relationship between conductivity and concentration of NaCl in PAA solution at 20 °C.

It is well known that PAA is a medium-strong acid, and the conductivity of low concentration of PAA is rather lower. When NaCl is added into PAA solution, NaCl can dissociate into sodium and chloride ions. These ions act as charge carriers and increase the conductivity of the solution. This truth also can be verified by Fig.8. Fig.8 gives the conductivity as a function of concentration of NaCl 20

°C, it is apparent that the conductivity linearly increases with increase of the concentration of NaCl. Since corrosion is an electrochemical process, increased conductivity increases the rate at which the metal is oxidized, and corrosion accelerates. Thus, the corrosion of CRS in PAA solution can be accelerated by addition of NaCl.

On the other hand, NaCl can accelerate the anodic and cathodic reactions based on the following mechanism [30].

In anodic sides:

$$Fe+mH_2O + Cl^- = FeClOH^-{}_{ads} + (m-1)H_2O + H^+ +e^- \qquad (a)$$

$$FeClOH^-{}_{ads} = FeClOH +e^- \qquad (b)$$

$$FeClOH + H^+ = Fe^{2+} + Cl^- + H_2O \qquad (c)$$

In cathodic sides:

$$Fe + H^+ + Cl^- + e^- = (H\text{-}Fe\text{-}Cl^-)_{ads} \qquad (d)$$

$$2(H\text{-}Fe\text{-}Cl^-)_{ads} = (H\text{-}Fe\text{-}H)_{ads} +FeCl^- + Cl^- \qquad (e)$$

$$(H\text{-}Fe\text{-}H)_{ads} = Fe + H_2 \qquad (f)$$

$$FeCl^- = Fe + Cl^- \qquad (g)$$

It is apparent that both the anodic and cathodic reactions can be accelerated by chloride ion. This hypothesis is consistent with the results observed from polarization curves. In the above mechanism, the adsorption of chloride ion on steel surface is the rate – determining step. With increasing the concentration of NaCl, the adsorption reactions will be accelerated, suggesting that the anodic and cathodic reactions can be accelerated with increasing the concentration of NaCl.

However, according to the mechanism for CRS in PAA suggested by Qu et al [7-9], the anodic dissolution of CRS in PAA solutions in the absence of NaCl may be assumed as follows:

$$CH_3COOOH = CH_3COOO^- + H^+ \qquad (h)$$

$$Fe + CH_3COOO^- = [Fe(CH_3COOO^-)]_{ads} \qquad (i)$$

$$[Fe(CH_3COOO^-)]_{ads} = [Fe(CH_3COOO)] + e^- \qquad (j)$$

$$[Fe(CH_3COOO)] = [Fe(CH_3COOO)]^+ + e^- \qquad (k)$$

$$[Fe(CH_3COOO)]^+ = Fe^{2+} + CH_3COOO^- \qquad (l)$$

The adsorption of CH_3COOO^- ions on the surface of CRS to form the $[Fe(CH_3COOO^-)]_{ads}$ film is the prerequisite for the anodic dissolution. But it can not create compact film on CRS surface due to the electrostatic repulsion interaction among CH_3COOO^- ions. Thus, chloride ions are likely to thrill through the interval of the adsorption film of CH_3COOO^- and adsorb onto CRS surface because the radius of chloride ion is very tiny. So a small quantity of chloride ions can accelerate the corrosion of CRS in PAA. However, when the concentration of chloride ions is higher than a certain critical concentration, due to the electrostatic repulsion interaction, the adsorbed chloride ions and CH_3COOO^- ions will further hinders the physical contact of the superfluous chloride ions with the metal-solution interface. Additionally, with increasing the concentration of chloride ions, the reduction ability of chloride ions also increases, consequently, the following reaction may occurs in PAA solution.

$$CH_3COOO^- + 2Cl^- + 2H^+ = CH_3COO^- + H_2O + Cl_2\uparrow \qquad (m)$$

Reaction (m) will decrease the concentration of PAA and chloride, so the corrosion of CRS is depressed somewhat with chloride level higher than the threshold value. This may be why the maximum corrosion rate only appears in the presence of 0.005 M NaCl in PAA.

5. CONCLUSION

1. Test temperatures can affect the corrosion rate of CRS in PAA clearly. At each same concentration of NaCl, the corrosion increases with increasing the temperature.
2. NaCl concentration has a critical influence on the corrosion rate of CRS in PAA solution. The corrosion rate firstly increases with increasing chloride content up to a certain critical concentration (0.005 M), and then decreases in solution with chloride level higher than the threshold value at each same temperature.
3. Chloride ions do not provoke the pitting corrosion of CRS in PAA solution.
4. The corrosion of CRS in PAA is due to the cooperation of chloride ions and PAA ions.

ACKNOWLEDGEMENTS
This work was financially supported by Chinese Natural Science Foundation under the Grant No. 51161025, No. 21162036, No. 50761007 and No.20762014.

References

1. H.C. Flemming, Zentralbl. *Bakteriol. Mikrobiol. Hyg*. [B] 197 (1984) 97.
2. M. Mari, T. Cembali, E. Baraldi, L. Casalini, *Plant Dis*. 83 (1999)773.
3. E.M.M. Rossoni, C.C. Gaylarde, *Int. J. Food Microbiol*. 61 (2000) 81.
4. M. Kitis, *Environ. Int*. 30 (2004) 47.
5. A. Dell Erba, D. Falsanisi, L. Liberti, M. Notarnicola, D. Santoro, *Desalination* 168(2004) 435.
6. A. Pehkonen, T. Salo, J. Aromaa, O. Forsen, *Pulp Pap. – Can*. 101 (2000) 46.
7. Q. Qu, S. Jiang, L. Li, W. Bai, J. Zhou, *Corros. Sci*. 50 (2008) 35.

8. Q. Qu, L. Li, S. Jiang, W. Bai, Z. Ding, *J. Appl. Electrochem*. 39 (2009) 569.
9. Q. Qu, L. Li, W. Bai, S. Jiang, Z. Ding, *Corros. Sci*. 51 (2009) 2423.
10. H. H. Hassan, *Electrochem. Acta* 51[2005]526.
11. T. Szauer, A. Brandt, *Corros. Sci*. 23 (1983) 473.
12. C.A. Acosta, R.C. Salvarezza, H.H. Videla, A.J. Arvia, *Corros. Sci*. 25 (1985) 291.
13. N. Cui, H.Y. Ma, J.L. Luo, S. Chiovelli, *Electrochem. Commun*. 3(2001) 716.
14. M. Safira, A. Srhiri, M. Keddam, H. Takenouti, *Electrochim. Acta* 44 (1999) 4395.
15. F. El-Taib Heakal, N.S. Tantawy, O.S. Shehta, *Mater. Chem. Phys*. 130(2011)743.
16. T.Murakawa, S.Nagaura, N.Hackerman.*Corros. Sci*., 7 (1967) 79
17. X. Li, L. Tang, *Corros. Sci*., 48(2006)308-321
18. C.T. Lee, Z. Qin, M. Odziemkowski, D.W. Shoesmith, *Electrochim. Acta* 51 (2006) 1558
19. L.A. De Faria, J.F.C. Boodts, S. Trasatti, *J. Appl. Electrochem*. 26 (1996) 1195.
20. N.T. Krstajic, S. Trasatti, *J. Appl. Electrochem*. 28(1998) 129.
21. A. Kapalka, G. Fóti, C. Comninellis, *Electrochem. Commun*. 10(2008) 607.
22. G. Rocchini, *Corros. Sci*. 38 (1996) 655.
23. W. Oelssner, F. Berthold, U. Guth, *Mater. Corros*. 57 (2006) 455
24. L. Larabi, Y. Harek, M. Traisnel, A. Mansri, *J. Appl. Electrochem*. 34 (2004) 833.
25. C. Jeyaprabha, S. Sathiyanarayanan, G. Venkatachari, *J. Appl. Polym. Sci*. 101 (2006) 2144.
26. W.A. Badawy, K.M. Ismail, A.M. Fathi, *Electrochim. Acta* 51 (2006) 4182.
27. M.A. Veloz, I. González, *Electrochim. Acta* 48(2002) 135.
28. P. Bommersbach, C. Alemany-Dumont, *Electrochim. Acta* 51 (2006)4011.
29. M. Lagrenée, B. Mernari, M. Bouanis, M. Traisnel, F. Bentiss, *Corros. Sci*. 44 (2002) 573.
30. J.H. Dong, C.N. Cao, H.C. Lin, *Acta Phys.-Chim*. 11(1995)279